

UC Berkeley

UC Berkeley Previously Published Works

Title

Measurement of $\Upsilon(1S)$ Elliptic Flow at Forward Rapidity in Pb-Pb Collisions at $\sqrt{s_{NN}}=5.02$ TeV

Permalink

<https://escholarship.org/uc/item/8bg7s54h>

Journal

Physical Review Letters, 123(19)

ISSN

0031-9007

Authors

Acharya, S
Adamová, D
Adhya, SP
[et al.](#)

Publication Date

2019-11-08

DOI

10.1103/physrevlett.123.192301

Peer reviewed

Measurement of $\Upsilon(1S)$ Elliptic Flow at Forward Rapidity in Pb-Pb Collisions at $\sqrt{s_{NN}} = 5.02$ TeV

S. Acharya *et al.**

(A Large Ion Collider Experiment Collaboration)

 (Received 15 July 2019; revised manuscript received 9 September 2019; published 6 November 2019)

The first measurement of the $\Upsilon(1S)$ elliptic flow coefficient (v_2) is performed at forward rapidity ($2.5 < y < 4$) in Pb–Pb collisions at $\sqrt{s_{NN}} = 5.02$ TeV with the ALICE detector at the LHC. The results are obtained with the scalar product method and are reported as a function of transverse momentum (p_T) up to 15 GeV/ c in the 5%–60% centrality interval. The measured $\Upsilon(1S)v_2$ is consistent with 0 and with the small positive values predicted by transport models within uncertainties. The v_2 coefficient in $2 < p_T < 15$ GeV/ c is lower than that of inclusive J/ψ mesons in the same p_T interval by 2.6 standard deviations. These results, combined with earlier suppression measurements, are in agreement with a scenario in which the $\Upsilon(1S)$ production in Pb–Pb collisions at LHC energies is dominated by dissociation limited to the early stage of the collision, whereas in the J/ψ case there is substantial experimental evidence of an additional regeneration component.

DOI: [10.1103/PhysRevLett.123.192301](https://doi.org/10.1103/PhysRevLett.123.192301)

At the extreme energy densities and temperatures produced in ultrarelativistic collisions of heavy nuclei, hadronic matter undergoes a transition into a state of deconfined quarks and gluons, known as quark-gluon plasma (QGP). The created QGP medium is characterized as a strongly coupled system, which behaves as an almost perfect fluid in the sense that its shear viscosity to entropy density ratio approaches the smallest possible values [1–3]. Spatial initial state anisotropy of the overlap region of the two colliding nuclei is transformed by the fluid pressure gradients into a momentum anisotropy of the produced final-state particles. This effect is known as hydrodynamic anisotropic flow [4] and is usually quantified in terms of the harmonic coefficients of the Fourier decomposition of the azimuthal particle distribution [5]. The dominant coefficient in noncentral collisions is the second harmonic, denoted by v_2 and known as elliptic flow, since this coefficient directly arises from the almond-shaped interaction region between the colliding nuclei. It is approximately proportional to the eccentricity e_2 of the initial collision geometry [6]. The proportionality coefficient reflects the response of the QGP medium to the initial anisotropy and depends on the particle type, mass, and kinematics [7].

Charm and beauty quarks are important probes of the QGP. They are created predominantly in hard-scattering processes at the early collision stage and therefore experience the entire evolution of the QGP. The observed significant D meson v_2 in nucleus-nucleus collisions suggests that the charm quarks participate in the collective anisotropic flow of the QGP fluid [8–10]. Nevertheless, since the light-flavor quarks also contribute to the D -meson flow, detailed comparisons with theoretical models are necessary to draw firm conclusions about the charm-quark flow. Quarkonia, which are bound states of heavy-flavor quark-antiquark pairs, offer a complementary way to study the interaction of the heavy-flavor quarks with the medium and thus to independently shed light on the properties of the QGP [11]. In a simplified picture, quarkonium production is suppressed by color screening inside the QGP medium created in nucleus-nucleus collisions [12]. The level of suppression depends on the heavy-quark interaction and the temperature of the surrounding medium [13,14]. The azimuthal asymmetry of the overlap region of the two colliding nuclei and the dependence of the suppression on the path length traversed by the quark-antiquark pair inside the medium lead to positive v_2 values increasing as a function of transverse momentum (p_T). At LHC energies, there is evidence for a competing effect that enhances the production of charmonia (bound states of charm quark-antiquark pairs) [15–17]. This effect originates from regeneration of charmonia via recombination of (partially) thermalized charm quarks either during the QGP evolution [18,19] or at the QGP phase boundary [20,21]. It becomes significant at LHC energies due to the large charm-quark production cross section, which implies that a sufficiently

*Full author list given at the end of the article.

Published by the American Physical Society under the terms of the [Creative Commons Attribution 4.0 International license](https://creativecommons.org/licenses/by/4.0/). Further distribution of this work must maintain attribution to the author(s) and the published article's title, journal citation, and DOI.

high number of charm quarks traveling inside the QGP are available for recombination. Within the regeneration scenario, the elliptic flow of charmonia is directly inherited from the velocity field of the individual charm quarks within the medium and results in a positive v_2 coefficient, mainly at low p_T . Measurements of significant J/ψ -meson v_2 coefficient in Pb-Pb collisions at LHC energies clearly speak in favor of charm-quark flow and the regeneration scenario [22–25]. Despite this, the phenomenological models that incorporate transport of heavy-flavor quark-antiquark pairs inside the QGP are not yet able to provide a fully satisfactory description of the p_T dependence of the measured J/ψ elliptic flow [19,26]. Moreover, recent results in high-multiplicity p -Pb collisions also indicate a significant $J/\psi v_2$ [27,28], which is unexpected within the present transport models due to the small collision-system size and low number of available charm quarks [29]. Recent calculations within the color-glass condensate framework attribute this significant v_2 to initial-state effects [30].

Bottomonia, bound states of bottom quark-antiquark pairs, are also expected to be suppressed inside the QGP by the color-screening effect [11,13,31]. Indeed, measurements in Pb-Pb collisions at the LHC demonstrate a significant suppression of inclusive $\Upsilon(1S)$ production [32–35]. In recent calculations the v_2 coefficient of inclusive $\Upsilon(1S)$ is predicted to be significantly smaller when compared to that of inclusive J/ψ [36]. The reason is that the $\Upsilon(1S)$ dissociation happens at higher temperatures due to its greater binding energy. The dissociation is therefore limited to the earlier stage of the collision, when the path-length differences are less influential. In addition, the recombination of (partially) thermalized bottom quarks gives a negligible contribution to the v_2 coefficient due to the small number of available bottom quarks [36]. As a result, the predicted values of $\Upsilon(1S)$ v_2 coefficient are small in contrast to the charmonium case. It is worth noting that even though the v_2 coefficient of the excited bottomonium state $\Upsilon(2S)$ is currently beyond experimental reach, it is expected to be significantly higher than that of $\Upsilon(1S)$. Because of its lower binding energy and other bound-state characteristic differences, the suppression and regeneration occur up to a later stage of the collision. Hence, the path-length dependent suppression induces a larger v_2 , the fraction of regenerated $\Upsilon(2S)$ is higher, and the inherited v_2 is larger [36]. Consequently, the measurement of the bottomonium elliptic flow is a crucial ingredient in the study of heavy-flavor interactions with the QGP, not only to complement the corresponding charmonium measurements, but also in the search for any sizable v_2 beyond the theoretical expectations.

In this Letter, we present the first measurement of $\Upsilon(1S)$ elliptic flow in Pb-Pb collisions at $\sqrt{s_{NN}} = 5.02$ TeV at forward rapidity ($2.5 < y < 4$). The Υ mesons are reconstructed via their $\mu^+\mu^-$ decay channel. The results are

obtained in the momentum interval $0 < p_T < 15$ GeV/ c and the 5%–60% collision centrality interval.

General information on the ALICE apparatus and its performance can be found in Refs. [37,38]. The muon spectrometer, which covers the pseudorapidity range $-4 < \eta < -2.5$, is used to reconstruct muon tracks. (In the ALICE reference frame, the muon spectrometer covers a negative η range and consequently a negative y range. The results were chosen to be presented with a positive y notation, due to the symmetry of the collision system.) It consists of a front absorber followed by five tracking stations with the third station placed inside a dipole magnet. Two trigger stations located downstream of an iron wall complete the spectrometer. The silicon pixel detector (SPD) [39,40] consists of two cylindrical layers covering the full azimuthal angle and $|\eta| < 2.0$ and $|\eta| < 1.4$, respectively. The SPD is employed to determine the position of the primary vertex and to reconstruct tracklets, track segments formed by the clusters in the two SPD layers and the primary vertex [41]. Two arrays of 32 scintillator counters each [42], covering $2.8 < \eta < 5.1$ (V0A) and $-3.7 < \eta < -1.7$ (V0C), are used for triggering, the event selection, and the determination of the collision centrality and the event flow vector. In addition, two neutron zero degree calorimeters [43], installed 112.5 m from the interaction point along the beam line on each side, are employed for the event selection.

The data samples recorded by ALICE during the 2015 and 2018 LHC Pb-Pb runs at $\sqrt{s_{NN}} = 5.02$ TeV are used for this analysis. The trigger conditions and the event selection criteria are described in Ref. [24]. The primary vertex position is required to be within ± 14 cm from the nominal interaction point along the beam direction. The data are split in intervals of collision centrality, which is obtained based on the total signal in the V0A and V0C detectors [44]. The integrated luminosity of the analyzed data sample is about $750 \mu\text{b}^{-1}$.

The muon selection is identical to that used in Refs. [24,27]. The dimuons are reconstructed in the acceptance of the muon spectrometer ($2.5 < y < 4.0$) and are required to have a transverse momentum between 0 and 15 GeV/ c . The alignment of the muon spectrometer is performed based on the MILLEPEDE package [45] and using Pb-Pb data taken with the nominal dipole magnetic field [38]. The presence of the magnetic field limits the precision of the alignment procedure in the track bending direction. Indeed, a study of the reconstructed Υ mass as a function of the momentum of muon tracks (p_μ) reveals a residual misalignment leading to a systematic shift in the measured muon track momentum $\Delta(1/p_\mu) \approx \pm 2.5 \times 10^{-4} (\text{GeV}/c)^{-1}$, where the sign of the shift depends on the muon charge and the magnetic field polarity. A correction of this misalignment effect is obtained via a high-statistics sample of reconstructed $J/\psi \rightarrow \mu^+\mu^-$ decays and the spectra of high-momentum muon tracks.

The correction is then applied to the reconstructed muon track momentum, resulting in up to 25% improvement of the $\Upsilon(1S)$ mass resolution for $p_T > 6$ GeV/ c .

The dimuon invariant mass ($M_{\mu\mu}$) distribution is fitted with a combination of an extended crystal ball (CB2) function for the $\Upsilon(1S)$ signal and a variable-width Gaussian function with a quadratic dependence of the width on $M_{\mu\mu}$ for the background [46]. A binned maximum-likelihood fit is employed. The $\Upsilon(1S)$ peak position and width are left free, while the CB2 tail parameters are fixed to the values extracted from Monte Carlo simulations [35]. The $\Upsilon(2S)$ and $\Upsilon(3S)$ signals are included in the fit. Their peak positions and widths are fixed to those of the $\Upsilon(1S)$ scaled by the ratio of their nominal masses to the nominal mass of the $\Upsilon(1S)$. An example of the $M_{\mu\mu}$ fit is shown in the left panel of Fig. 1. It is worth noting that no statistically significant $\Upsilon(3S)$ is observed in any of the studied centrality and p_T intervals, and thus it is not considered in the further analysis.

The dimuon v_2 is measured using the scalar product method [47,48], correlating the reconstructed dimuons with the second-order harmonic event flow vector $\mathbf{Q}_2^{\text{SPD}}$ [5,49] calculated from the azimuthal distribution of the reconstructed SPD tracklets

$$v_2\{\text{SP}\} = \left\langle \mathbf{u}_2 \mathbf{Q}_2^{\text{SPD}*} \middle/ \sqrt{\frac{\langle \mathbf{Q}_2^{\text{SPD}} \mathbf{Q}_2^{\text{V0A}*} \rangle \langle \mathbf{Q}_2^{\text{SPD}} \mathbf{Q}_2^{\text{V0C}*} \rangle}{\langle \mathbf{Q}_2^{\text{V0A}} \mathbf{Q}_2^{\text{V0C}*} \rangle}} \right\rangle_{\mu\mu}, \quad (1)$$

where $\mathbf{u}_2 = \exp(i2\varphi)$ is the unit flow vector of the dimuon with azimuthal angle φ . The brackets $\langle \dots \rangle_{\mu\mu}$ denote an average over all dimuons belonging to a given p_T , $M_{\mu\mu}$ and centrality interval. The $\mathbf{Q}_2^{\text{V0A}}$ and $\mathbf{Q}_2^{\text{V0C}}$ are the event flow vectors calculated from the azimuthal distribution of the

energy deposition measured in the V0A and V0C detectors, respectively, and $*$ is the complex conjugate. The brackets $\langle \dots \rangle$ in the denominator denote an average over all events in a sufficiently narrow centrality class that encloses the event containing the dimuon. In order to account for a nonuniform detector response and efficiency, the components of all three event flow vectors are corrected using a recentering procedure [50]. The gaps in pseudorapidity between the muon spectrometer and SPD ($|\Delta\eta| > 1.0$) and between the SPD, V0A, and V0C remove autocorrelations and suppress short-range correlations unrelated to the azimuthal asymmetry in the initial geometry (“nonflow”), which largely come from jets and resonance decays. In the following, the $v_2\{\text{SP}\}$ coefficient is denoted as v_2 .

The $\Upsilon(1S)v_2$ coefficient is obtained by a least squares fit of the superposition of the $\Upsilon(1S)$ signal and the background to the dimuon flow coefficient as a function of the dimuon invariant mass [51]

$$v_2(M_{\mu\mu}) = \alpha(M_{\mu\mu})v_2^{\Upsilon(1S)} + [1 - \alpha(M_{\mu\mu})]v_2^B(M_{\mu\mu}), \quad (2)$$

where $v_2^{\Upsilon(1S)}$ is the flow coefficient of the signal, v_2^B is the $M_{\mu\mu}$ -dependent flow coefficient of the background, and $\alpha(M_{\mu\mu})$ is the signal fraction, obtained from the fit of the $M_{\mu\mu}$ distribution described above. The background v_2^B is modeled as a second-order polynomial function of $M_{\mu\mu}$. For consistency, and despite its low yield, the $\Upsilon(2S)$ is included in the fit by restricting the value of its v_2 coefficient within the range between -0.5 and 0.5 . In practice, this inclusion has a negligible impact on the $\Upsilon(1S)$ fit results. An example of $v_2(M_{\mu\mu})$ fit is presented in the right panel of Fig. 1.

The main systematic uncertainty of the measurement arises from the choice of the background fit function $v_2^B(M_{\mu\mu})$. In order to estimate this uncertainty, linear and constant functions are also used instead of the second-order

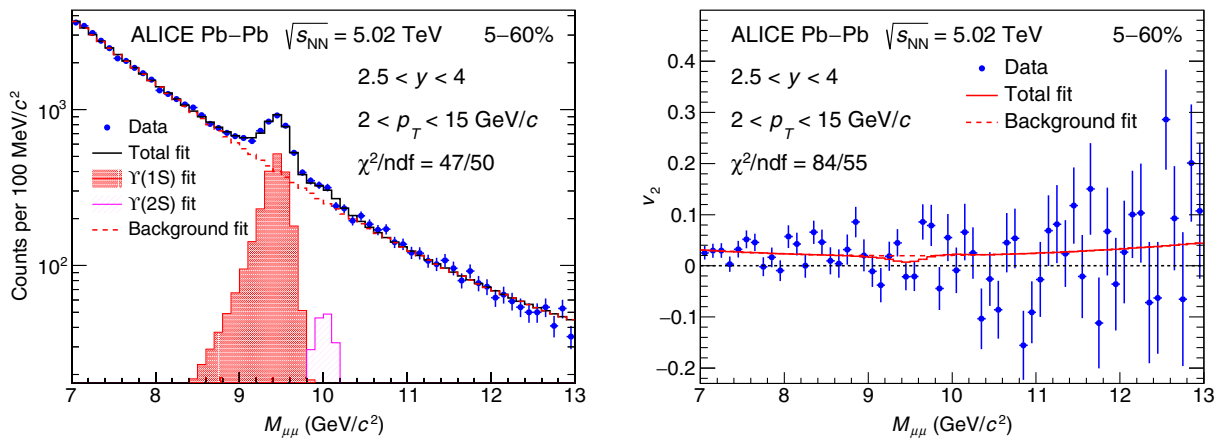


FIG. 1. Left: The $M_{\mu\mu}$ distribution in the 5%–60% centrality interval and $2 < p_T < 15$ GeV/ c fitted with a combination of an extended crystal ball function for the signal and a variable-width Gaussian function for the background. Right: The $v_2(M_{\mu\mu})$ distribution in the same centrality and p_T intervals fitted with the function from Eq. (2).

polynomial. In addition, the signal CB2 tail parameters and background fit functions are varied [35]. The systematic uncertainty is then derived as the standard deviation with respect to the default choice of fitting functions. The absolute uncertainty increases from 0.004 to 0.016 with increasing collision centrality and decreasing p_T , which is due to the decreasing signal-to-background ratio. The dimuon trigger and reconstruction efficiency depends on the detector occupancy. This, coupled to the muon flow, could lead to a bias in the measured v_2 . The corresponding systematic uncertainty is obtained by embedding simulated $\Upsilon(1S)$ decays into real Pb-Pb events [24]. It is found to be at most 0.0015 and is conservatively assumed to be the same in all transverse momentum and centrality intervals. The variations of the fit range and invariant-mass binning do not lead to deviations beyond the expected statistical fluctuations. The uncertainty related to the magnitude of the $\mathbf{Q}_2^{\text{SPD}}$ flow vector is found to be negligible. Furthermore, the absence of any residual nonuniform detector acceptance and efficiency in the SPD flow vector determination after applying the recentering procedure is verified via the imaginary part of the scalar product [see Eq. (1)] [50].

Figure 2 shows the $\Upsilon(1S)$ v_2 coefficient as a function of transverse momentum in the 5%–60% centrality interval. The central (0%–5%) and peripheral (60%–100%) collisions are not considered as the eccentricity of the initial collision geometry is small for the former and the signal yield is low in the latter. The p_T intervals are 0–3, 3–6, and 6–15 GeV/ c and the points are located at the average transverse momentum of the reconstructed $\Upsilon(1S)$

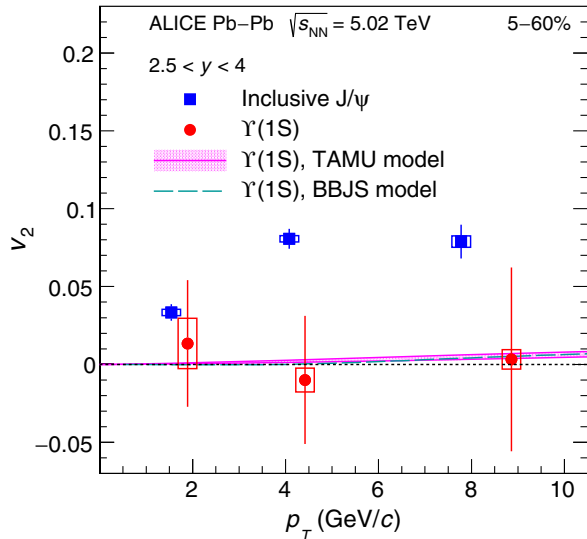


FIG. 2. The $\Upsilon(1S)$ v_2 coefficient as a function of p_T in the 5%–60% centrality interval compared to that of inclusive J/ψ . The cyan dashed line represents the BBJS model calculations [52], while the magenta band denotes the TAMU model calculations [36]. Error bars (open boxes) represent the statistical (systematic) uncertainties.

uncorrected for detector acceptance and efficiency. The results are compatible with 0 and with the small positive values predicted by the available theoretical models within uncertainties. The BBJ model calculations consider only the path-length dependent dissociation of initially created bottomonia inside the QGP medium [52]. The TAMU model incorporates in addition a regeneration component originating from the recombination of (partially) thermalized bottom quarks [36]. Given that the regeneration component gives practically negligible contribution to the total $\Upsilon(1S)$ v_2 , the differences between the two models are marginal. It is worth noting that although the quoted model predictions are for midrapidity, they remain valid also for the rapidity range of the measurement within the theoretical uncertainties. Indeed the fractions of regenerated and initially produced $\Upsilon(1S)$ are very close at mid and forward rapidities [36]. In addition, the QGP medium evolution is also similar between mid and forward rapidities, given the weak rapidity dependence of the charged-particle multiplicity density [53]. The presented $\Upsilon(1S)$ v_2 result is coherent with the measured $\Upsilon(1S)$ suppression in Pb-Pb collisions [35], as the level of suppression is also fairly well reproduced by the BBJ model and the TAMU model including or excluding a regeneration component. Therefore, the result is in agreement with a scenario in which the predominant mechanism affecting $\Upsilon(1S)$ production in Pb-Pb collisions at the LHC energies is the dissociation limited to the early stage of the collision. It is interesting to note that the presented $\Upsilon(1S)$ v_2 results are reminiscent of the corresponding charmonia measurements in Au-Au collisions at RHIC [54], where so far non-observation of significant v_2 is commonly interpreted as a sign of a small regeneration component from recombination of thermalized charm quarks at lower RHIC energies.

The $\Upsilon(1S)$ v_2 values in the three p_T intervals shown in Fig. 2 are found to be lower, albeit with large uncertainties, compared to those of the inclusive J/ψ measured in the same centrality and p_T intervals using the data sample and analysis procedure described in Ref. [24]. Given that any v_2 originating either from recombination or from path-length dependent dissociation vanishes at zero p_T , the observed difference between $\Upsilon(1S)$ and $J/\psi v_2$ is quantified by performing the p_T -integrated measurement excluding the low p_T range. Figure 3 presents the $\Upsilon(1S)$ v_2 coefficient integrated over the transverse momentum range $2 < p_T < 15$ GeV/ c for three centrality intervals compared with that of the inclusive J/ψ . The $\Upsilon(1S)$ v_2 is found to be $-0.003 \pm 0.030(\text{stat}) \pm 0.006(\text{syst})$ in the $2 < p_T < 15$ GeV/ c and 5%–60% centrality interval. This value is lower than the corresponding $J/\psi v_2$ by 2.6σ . This observation, coupled to the different measured centrality and p_T dependence of the $\Upsilon(1S)$ and J/ψ suppression in Pb-Pb collisions at the LHC [17,35], can be interpreted within the models used for comparison as a sign that unlike $\Upsilon(1S)$, J/ψ production has a significant regeneration component.

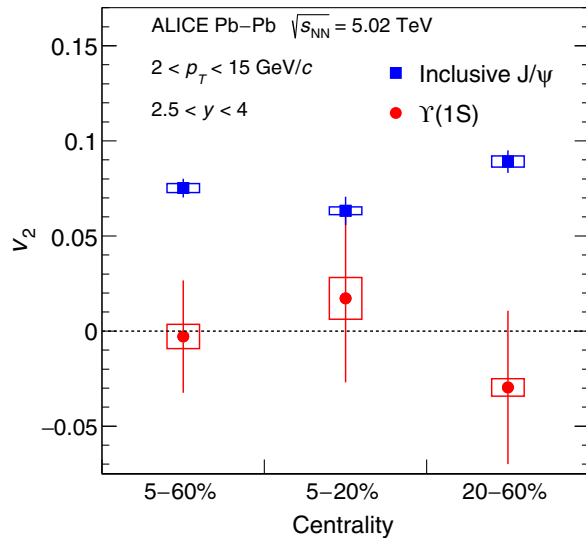


FIG. 3. The $\Upsilon(1S)$ v_2 coefficient integrated over the transverse momentum range $2 < p_T < 15$ GeV/c in three centrality intervals compared to that of inclusive J/ψ . Error bars (open boxes) represent the statistical (systematic) uncertainties.

Nevertheless, no firm conclusions can be drawn, given that currently the transport models cannot explain the significant $J/\psi v_2$ for $p_T > 4-5$ GeV/c observed in the data [23].

In summary, the first measurement of the $\Upsilon(1S)$ v_2 coefficient in Pb-Pb collisions at $\sqrt{s_{NN}} = 5.02$ TeV is presented. The measurement is performed in the 5%–60% centrality interval within $0 < p_T < 15$ GeV/c range at forward rapidity. The v_2 coefficient is compatible with 0 and with the model predictions within uncertainties. Excluding low p_T ($0 < p_T < 2$ GeV/c), $\Upsilon(1S)$ v_2 is found to be 2.6σ lower with respect to that of inclusive J/ψ . The presented measurement opens the way for further studies of bottomonium flow using the future data samples from the LHC Runs 3 and 4 with an expected tenfold increase in the number of the Υ candidates [55,56].

The ALICE Collaboration thanks all its engineers and technicians for their invaluable contributions to the construction of the experiment and the CERN accelerator teams for the outstanding performance of the LHC complex. The ALICE Collaboration gratefully acknowledges the resources and support provided by all Grid centres and the Worldwide LHC Computing Grid (WLCG) collaboration. The ALICE Collaboration acknowledges the following funding agencies for their support in building and running the ALICE detector: A. I. Alikhanyan National Science Laboratory (Yerevan Physics Institute) Foundation (ANSL), State Committee of Science and World Federation of Scientists (WFS), Armenia; Austrian Academy of Sciences, Austrian Science Fund (FWF): [M 2467-N36] and Nationalstiftung für Forschung, Technologie und Entwicklung, Austria; Ministry of Communications and High Technologies, National Nuclear Research Center,

Azerbaijan; Conselho Nacional de Desenvolvimento Científico e Tecnológico (CNPq), Universidade Federal do Rio Grande do Sul (UFRGS), Financiadora de Estudos e Projetos (Finep) and Fundação de Amparo à Pesquisa do Estado de São Paulo (FAPESP), Brazil; Ministry of Science & Technology of China (MSTC), National Natural Science Foundation of China (NSFC) and Ministry of Education of China (MOEC), China; Croatian Science Foundation and Ministry of Science and Education, Croatia; Centro de Aplicaciones Tecnológicas y Desarrollo Nuclear (CEADEN), Cubaenergía, Cuba; Ministry of Education, Youth and Sports of the Czech Republic, Czech Republic; The Danish Council for Independent Research | Natural Sciences, the Carlsberg Foundation and Danish National Research Foundation (DNRF), Denmark; Helsinki Institute of Physics (HIP), Finland; Commissariat à l’Energie Atomique (CEA), Institut National de Physique Nucléaire et de Physique des Particules (IN2P3) and Centre National de la Recherche Scientifique (CNRS) and Région des Pays de la Loire, France; Bundesministerium für Bildung und Forschung (BMBF) and GSI Helmholtzzentrum für Schwerionenforschung GmbH, Germany; General Secretariat for Research and Technology, Ministry of Education, Research and Religions, Greece; National Research, Development and Innovation Office, Hungary; Department of Atomic Energy Government of India (DAE), Department of Science and Technology, Government of India (DST), University Grants Commission, Government of India (UGC) and Council of Scientific and Industrial Research (CSIR), India; Indonesian Institute of Science, Indonesia; Centro Fermi—Museo Storico della Fisica e Centro Studi e Ricerche Enrico Fermi and Istituto Nazionale di Fisica Nucleare (INFN), Italy; Institute for Innovative Science and Technology, Nagasaki Institute of Applied Science (IIST), Japan Society for the Promotion of Science (JSPS) KAKENHI and Japanese Ministry of Education, Culture, Sports, Science and Technology (MEXT), Japan; Consejo Nacional de Ciencia (CONACYT) y Tecnología, through Fondo de Cooperación Internacional en Ciencia y Tecnología (FONCICYT) and Dirección General de Asuntos del Personal Académico (DGAPA), Mexico; Nederlandse Organisatie voor Wetenschappelijk Onderzoek (NWO), Netherlands; The Research Council of Norway, Norway; Commission on Science and Technology for Sustainable Development in the South (COMSATS), Pakistan; Pontificia Universidad Católica del Perú, Peru; Ministry of Science and Higher Education and National Science Centre, Poland; Korea Institute of Science and Technology Information and National Research Foundation of Korea (NRF), Republic of Korea; Ministry of Education and Scientific Research, Institute of Atomic Physics and Ministry of Research and Innovation and Institute of Atomic Physics, Romania; Joint Institute for Nuclear Research (JINR), Ministry of

Education and Science of the Russian Federation, National Research Centre Kurchatov Institute, Russian Science Foundation and Russian Foundation for Basic Research, Russia; Ministry of Education, Science, Research and Sport of the Slovak Republic, Slovakia; National Research Foundation of South Africa, South Africa; Swedish Research Council (VR) and Knut & Alice Wallenberg Foundation (KAW), Sweden; European Organization for Nuclear Research, Switzerland; National Science and Technology Development Agency (NSDTA), Suranaree University of Technology (SUT) and Office of the Higher Education Commission under NRU project of Thailand, Thailand; Turkish Atomic Energy Agency (TAEK), Turkey; National Academy of Sciences of Ukraine, Ukraine; Science and Technology Facilities Council (STFC), United Kingdom; National Science Foundation of the United States of America (NSF) and United States Department of Energy, Office of Nuclear Physics (DOE NP), United States of America.

-
- [1] P. K. Kovtun, D. T. Son, and A. O. Starinets, Viscosity in Strongly Interacting Quantum Field Theories from Black Hole Physics, *Phys. Rev. Lett.* **94**, 111601 (2005).
- [2] M. Luzum and P. Romatschke, Conformal relativistic viscous hydrodynamics: Applications to RHIC results at $\sqrt{s_{NN}} = 200$ GeV, *Phys. Rev. C* **78**, 034915 (2008); Erratum, *Phys. Rev. C* **79**, 039903(E) (2009).
- [3] P. Braun-Munzinger, V. Koch, T. Schaefer, and J. Stachel, Properties of hot and dense matter from relativistic heavy ion collisions, *Phys. Rep.* **621**, 76 (2016).
- [4] J.-Y. Ollitrault, Anisotropy as a signature of transverse collective flow, *Phys. Rev. D* **46**, 229 (1992).
- [5] S. Voloshin and Y. Zhang, Flow study in relativistic nuclear collisions by Fourier expansion of Azimuthal particle distributions, *Z. Phys. C* **70**, 665 (1996).
- [6] F. G. Gardim, F. Grassi, M. Luzum, and J.-Y. Ollitrault, Mapping the hydrodynamic response to the initial geometry in heavy-ion collisions, *Phys. Rev. C* **85**, 024908 (2012).
- [7] Z. Qiu and U. W. Heinz, Event-by-event shape and flow fluctuations of relativistic heavy-ion collision fireballs, *Phys. Rev. C* **84**, 024911 (2011).
- [8] S. Acharya *et al.* (ALICE Collaboration), D-Meson Azimuthal Anisotropy in Midcentral Pb-Pb Collisions at $\sqrt{s_{NN}} = 5.02$ TeV, *Phys. Rev. Lett.* **120**, 102301 (2018).
- [9] A. M. Sirunyan *et al.* (CMS Collaboration), Measurement of Prompt D^0 Meson Azimuthal Anisotropy in Pb-Pb Collisions at $\sqrt{s_{NN}} = 5.02$ TeV, *Phys. Rev. Lett.* **120**, 202301 (2018).
- [10] S. Acharya *et al.* (ALICE Collaboration), Event-shape engineering for the D-meson elliptic flow in midcentral Pb-Pb collisions at $\sqrt{s_{NN}} = 5.02$ TeV, *J. High Energy Phys.* **02** (2019) 150.
- [11] A. Andronic *et al.*, Heavy-flavour and quarkonium production in the LHC era: From proton-proton to heavy-ion collisions, *Eur. Phys. J. C* **76**, 107 (2016).
- [12] T. Matsui and H. Satz, J/ψ suppression by quark-gluon plasma formation, *Phys. Lett. B* **178**, 416 (1986).
- [13] S. Digal, P. Petreczky, and H. Satz, Quarkonium feed down and sequential suppression, *Phys. Rev. D* **64**, 094015 (2001).
- [14] A. Mocsy, P. Petreczky, and M. Strickland, Quarkonia in the quark gluon plasma, *Int. J. Mod. Phys. A* **28**, 1340012 (2013).
- [15] B. Abelev *et al.* (ALICE Collaboration), J/ψ Suppression at Forward Rapidity in Pb-Pb Collisions at $\sqrt{s_{NN}} = 2.76$ TeV, *Phys. Rev. Lett.* **109**, 072301 (2012).
- [16] B. B. Abelev *et al.* (ALICE Collaboration), Centrality, rapidity and transverse momentum dependence of J/ψ suppression in Pb-Pb collisions at $\sqrt{s_{NN}} = 2.76$ TeV, *Phys. Lett. B* **734**, 314 (2014).
- [17] J. Adam *et al.* (ALICE Collaboration), J/ψ suppression at forward rapidity in Pb-Pb collisions at $\sqrt{s_{NN}} = 5.02$ TeV, *Phys. Lett. B* **766**, 212 (2017).
- [18] M. He, R. J. Fries, and R. Rapp, Heavy flavor at the large hadron collider in a strong coupling approach, *Phys. Lett. B* **735**, 445 (2014).
- [19] X. Du and R. Rapp, Sequential regeneration of charmonia in heavy-ion collisions, *Nucl. Phys.* **A943**, 147 (2015).
- [20] P. Braun-Munzinger and J. Stachel, (Non)thermal aspects of charmonium production and a new look at J/ψ suppression, *Phys. Lett. B* **490**, 196 (2000).
- [21] A. Andronic, P. Braun-Munzinger, M. K. Koehler, and J. Stachel, Testing charm quark thermalisation within the statistical hadronisation model, *Nucl. Phys.* **A982**, 759 (2019).
- [22] E. Abbas *et al.* (ALICE Collaboration), J/ψ Elliptic Flow in Pb-Pb Collisions at $\sqrt{s_{NN}} = 2.76$ TeV, *Phys. Rev. Lett.* **111**, 162301 (2013).
- [23] S. Acharya *et al.* (ALICE Collaboration), J/ψ Elliptic Flow in Pb-Pb Collisions at $\sqrt{s_{NN}} = 5.02$ TeV, *Phys. Rev. Lett.* **119**, 242301 (2017).
- [24] S. Acharya *et al.* (ALICE Collaboration), Study of J/ψ azimuthal anisotropy at forward rapidity in Pb-Pb collisions at $\sqrt{s_{NN}} = 5.02$ TeV, *J. High Energy Phys.* **02** (2019) 012.
- [25] M. Aaboud *et al.* (ATLAS Collaboration), Prompt and nonprompt J/ψ elliptic flow in Pb + Pb collisions at $\sqrt{s_{NN}} = 5.02$ TeV with the ATLAS detector, *Eur. Phys. J. C* **78**, 784 (2018).
- [26] K. Zhou, N. Xu, Z. Xu, and P. Zhuang, Medium effects on charmonium production at ultrarelativistic energies available at the CERN large hadron collider, *Phys. Rev. C* **89**, 054911 (2014).
- [27] S. Acharya *et al.* (ALICE Collaboration), Search for collectivity with azimuthal J/ψ -hadron correlations in high multiplicity p-Pb collisions at $\sqrt{s_{NN}} = 5.02$ and 8.16 TeV, *Phys. Lett. B* **780**, 7 (2018).
- [28] A. M. Sirunyan *et al.* (CMS Collaboration), Observation of prompt J/ψ meson elliptic flow in high-multiplicity pPb collisions at $\sqrt{s_{NN}} = 8.16$ TeV, *Phys. Lett. B* **791**, 172 (2019).
- [29] X. Du and R. Rapp, In-medium charmonium production in proton-nucleus collisions, *J. High Energy Phys.* **03** (2019) 015.
- [30] C. Zhang, C. Marquet, G.-Y. Qin, S.-Y. Wei, and B.-W. Xiao, On the Elliptic Flow of Heavy Quarkonia in pA Collisions, *Phys. Rev. Lett.* **122**, 172302 (2019).

- [31] N. Brambilla *et al.*, Heavy quarkonium: Progress, puzzles, and opportunities, *Eur. Phys. J. C* **71**, 1534 (2011).
- [32] S. Chatrchyan *et al.* (CMS Collaboration), Observation of Sequential Upsilon Suppression in PbPb Collisions, *Phys. Rev. Lett.* **109**, 222301 (2012); Erratum, *Phys. Rev. Lett.* **120**, 199903(E) (2018).
- [33] B. B. Abelev *et al.* (ALICE Collaboration), Suppression of $\Upsilon(1S)$ at forward rapidity in Pb-Pb collisions at $\sqrt{s_{NN}} = 2.76$ TeV, *Phys. Lett. B* **738**, 361 (2014).
- [34] V. Khachatryan *et al.* (CMS Collaboration), Suppression of $\Upsilon(1S)$, $\Upsilon(2S)$ and $\Upsilon(3S)$ production in PbPb collisions at $\sqrt{s_{NN}} = 2.76$ TeV, *Phys. Lett. B* **770**, 357 (2017).
- [35] S. Acharya *et al.* (ALICE Collaboration), Υ suppression at forward rapidity in Pb-Pb collisions at $\sqrt{s_{NN}} = 5.02$ TeV, *Phys. Lett. B* **790**, 89 (2019).
- [36] X. Du, R. Rapp, and M. He, Color screening and regeneration of bottomonia in high-energy heavy-ion collisions, *Phys. Rev. C* **96**, 054901 (2017).
- [37] K. Aamodt *et al.* (ALICE Collaboration), The ALICE experiment at the CERN LHC, *J. Instrum.* **3**, S08002 (2008).
- [38] B. Abelev *et al.* (ALICE Collaboration), Performance of the ALICE experiment at the CERN LHC, *Int. J. Mod. Phys. A* **29**, 1430044 (2014).
- [39] G. Dellacasa *et al.* (ALICE Collaboration), ALICE technical design report of the inner tracking system (ITS), CERN Technical Report No. CERN-LHCC-99-012; ALICE-TDR-4, 1999, <https://cds.cern.ch/record/391175>.
- [40] K. Aamodt *et al.* (ALICE Collaboration), Alignment of the ALICE inner tracking system with cosmic-ray tracks, *J. Instrum.* **5**, P03003 (2010).
- [41] J. Adam *et al.* (ALICE Collaboration), Charged-particle multiplicities in proton-proton collisions at $\sqrt{s} = 0.9$ to 8 TeV, *Eur. Phys. J. C* **77**, 33 (2017).
- [42] E. Abbas *et al.* (ALICE Collaboration), Performance of the ALICE VZERO system, *J. Instrum.* **8**, P10016 (2013).
- [43] G. Dellacasa *et al.* (ALICE Collaboration), ALICE technical design report of the zero degree calorimeter (ZDC), CERN Technical Report No. CERN-LHCC-99-005; ALICE-TDR-3, 1999, <https://cds.cern.ch/record/381433>.
- [44] J. Adam *et al.* (ALICE Collaboration), Centrality Dependence of the Charged-Particle Multiplicity Density at Mid-rapidity in Pb-Pb Collisions at $\sqrt{s_{NN}} = 5.02$ TeV, *Phys. Rev. Lett.* **116**, 222302 (2016).
- [45] V. Blobel and C. Kleinwort, A new method for the high precision alignment of track detectors, in *Advanced Statistical Techniques in Particle Physics. Proceedings, Conference, Durham, UK* (University of Oxford, Oxford, 2002).
- [46] J. Adam *et al.* (ALICE Collaboration), Quarkonium signal extraction in ALICE, CERN Technical Report No. ALICE-PUBLIC-2015-006, 2015, <http://cds.cern.ch/record/2060096>.
- [47] C. Adler *et al.* (STAR Collaboration), Elliptic flow from two and four particle correlations in Au + Au collisions at $\sqrt{s_{NN}} = 130$ GeV, *Phys. Rev. C* **66**, 034904 (2002).
- [48] S. A. Voloshin, A. M. Poskanzer, and R. Snellings, Collective phenomena in noncentral nuclear collisions, *Landolt-Bornstein* **23**, 293 (2010).
- [49] J. Barrette *et al.* (E877 Collaboration), Observation of Anisotropic Event Shapes and Transverse Flow in Au + Au Collisions at AGS Energy, *Phys. Rev. Lett.* **73**, 2532 (1994).
- [50] I. Selyuzhenkov and S. Voloshin, Effects of nonuniform acceptance in anisotropic flow measurement, *Phys. Rev. C* **77**, 034904 (2008).
- [51] N. Borghini and J. Y. Ollitrault, Azimuthally sensitive correlations in nucleus-nucleus collisions, *Phys. Rev. C* **70**, 064905 (2004).
- [52] P. P. Bhaduri, N. Borghini, A. Jaiswal, and M. Strickland, Anisotropic escape mechanism and elliptic flow of bottomonia, [arXiv:1809.06235](https://arxiv.org/abs/1809.06235).
- [53] J. Adam *et al.* (ALICE Collaboration), Centrality dependence of the pseudorapidity density distribution for charged particles in Pb-Pb collisions at $\sqrt{s_{NN}} = 5.02$ TeV, *Phys. Lett. B* **772**, 567 (2017).
- [54] L. Adamczyk *et al.* (STAR Collaboration), Measurement of J/ψ Azimuthal Anisotropy in Au + Au Collisions at $\sqrt{s_{NN}} = 200$ GeV, *Phys. Rev. Lett.* **111**, 052301 (2013).
- [55] S. Acharya *et al.* (ALICE Collaboration), ALICE upgrade physics performance studies for 2018 report on HL/HE-LHC physics, CERN Technical Report No. ALICE-PUBLIC-2019-001, 2019, <http://cds.cern.ch/record/2661798>.
- [56] Z. Citron *et al.*, Future physics opportunities for high-density QCD at the LHC with heavy-ion and proton beams, in *HL/HE-LHC Workshop: Workshop on the Physics of HL-LHC, and Perspectives at HE-LHC Geneva, Switzerland* (CERN, Geneva 2018).

S. Acharya,¹⁴¹ D. Adamová,⁹³ S. P. Adhya,¹⁴¹ A. Adler,⁷³ J. Adolfsson,⁷⁹ M. M. Aggarwal,⁹⁸ G. Aglieri Rinella,³⁴ M. Agnello,³¹ N. Agrawal,^{10,48,53} Z. Ahammed,¹⁴¹ S. Ahmad,¹⁷ S. U. Ahn,⁷⁵ A. Akindinov,⁹⁰ M. Al-Turany,¹⁰⁵ S. N. Alam,¹⁴¹ D. S. D. Albuquerque,¹²² D. Aleksandrov,⁸⁶ B. Alessandro,⁵⁸ H. M. Alfanda,⁶ R. Alfaro Molina,⁷¹ B. Ali,¹⁷ Y. Ali,¹⁵ A. Alici,^{10,27a,27b,53} A. Alkin,² J. Alme,²² T. Alt,⁶⁸ L. Altenkamper,²² I. Altsybeev,¹¹² M. N. Anaam,⁶ C. Andrei,⁴⁷ D. Andreou,³⁴ H. A. Andrews,¹⁰⁹ A. Andronic,¹⁴⁴ M. Angeletti,³⁴ V. Angelov,¹⁰² C. Anson,¹⁶ T. Antičić,¹⁰⁶ F. Antinori,⁵⁶ P. Antonioli,⁵³ R. Anwar,¹²⁵ N. Apadula,⁷⁸ L. Aphecetche,¹¹⁴ H. Appelshäuser,⁶⁸ S. Arcelli,^{27a,27b} R. Arnaldi,⁵⁸ M. Arratia,⁷⁸ I. C. Arsene,²¹ M. Arslanodk,¹⁰² A. Augustinus,³⁴ R. Averbeck,¹⁰⁵ S. Aziz,⁶¹ M. D. Azmi,¹⁷ A. Badalà,⁵⁵ Y. W. Baek,⁴⁰ S. Bagnasco,⁵⁸ X. Bai,¹⁰⁵ R. Bailhache,⁶⁸ R. Bala,⁹⁹ A. Baldissieri,¹³⁷ M. Ball,⁴² S. Balouza,¹⁰³ R. C. Baral,⁸⁴ R. Barbera,^{28a,28b} L. Barioglio,^{26a,26b} G. G. Barnaföldi,¹⁴⁵ L. S. Barnby,⁹² V. Barret,¹³⁴ P. Bartalini,⁶ K. Barth,³⁴ E. Bartsch,⁶⁸ F. Baruffaldi,^{29a,29b} N. Bastid,¹³⁴ S. Basu,¹⁴³ G. Batigne,¹¹⁴ B. Batyunya,⁷⁴ P. C. Batzing,²¹ D. Bauri,⁴⁸ J. L. Bazo Alba,¹¹⁰

I. G. Bearden,⁸⁷ C. Bedda,⁶³ N. K. Behera,⁶⁰ I. Belikov,¹³⁶ F. Bellini,³⁴ R. Bellwied,¹²⁵ V. Belyaev,⁹¹ G. Bencedi,¹⁴⁵
 S. Beole,^{26a,26b} A. Bercuci,⁴⁷ Y. Berdnikov,⁹⁶ D. Berenyi,¹⁴⁵ R. A. Bertens,¹³⁰ D. Berzano,⁵⁸ M. G. Besoiu,⁶⁷ L. Betev,³⁴
 A. Bhasin,⁹⁹ I. R. Bhat,⁹⁹ M. A. Bhat,^{3a,3b} H. Bhatt,⁴⁸ B. Bhattacharjee,⁴¹ A. Bianchi,^{26a,26b} L. Bianchi,^{26a,26b} N. Bianchi,⁵¹
 J. Bielčík,³⁷ J. Bielčíková,⁹³ A. Bilandzic,^{103,117} G. Biro,¹⁴⁵ R. Biswas,^{3a,3b} S. Biswas,^{3a,3b} J. T. Blair,¹¹⁹ D. Blau,⁸⁶
 C. Blume,⁶⁸ G. Boca,¹³⁹ F. Bock,^{34,94} A. Bogdanov,⁹¹ L. Boldizsár,¹⁴⁵ A. Bolozdynya,⁹¹ M. Bombara,³⁸ G. Bonomi,¹⁴⁰
 H. Borel,¹³⁷ A. Borissof,^{91,144} M. Borri,¹²⁷ H. Bossi,¹⁴⁶ E. Botta,^{26a,26b} L. Bratrud,⁶⁸ P. Braun-Munzinger,¹⁰⁵ M. Bregant,¹²¹
 T. A. Broker,⁶⁸ M. Broz,³⁷ E. J. Brucken,⁴³ E. Bruna,⁵⁸ G. E. Bruno,^{33a,33b,104} M. D. Buckland,¹²⁷ D. Budnikov,¹⁰⁷
 H. Buesching,⁶⁸ S. Bufalino,³¹ O. Bugnon,¹¹⁴ P. Buhler,¹¹³ P. Buncic,³⁴ Z. Buthelezi,⁷² J. B. Butt,¹⁵ J. T. Buxton,⁹⁵
 S. A. Bysiak,¹¹⁸ D. Caffarri,⁸⁸ A. Caliva,¹⁰⁵ E. Calvo Villar,¹¹⁰ R. S. Camacho,⁴⁴ P. Camerini,^{25a,25b} A. A. Capon,¹¹³
 F. Carnesecchi,¹⁰ R. Caron,¹³⁷ J. Castillo Castellanos,¹³⁷ A. J. Castro,¹³⁰ E. A. R. Casula,⁵⁴ F. Catalano,³¹
 C. Ceballos Sanchez,⁵² P. Chakraborty,⁴⁸ S. Chandra,¹⁴¹ B. Chang,¹²⁶ W. Chang,⁶ S. Chapeland,³⁴ M. Chartier,¹²⁷
 S. Chattopadhyay,¹⁴¹ S. Chattopadhyay,¹⁰⁸ A. Chauvin,^{24a,24b} C. Cheshkov,¹³⁵ B. Cheynis,¹³⁵ V. Chibante Barroso,³⁴
 D. D. Chinellato,¹²² S. Cho,⁶⁰ P. Chochula,³⁴ T. Chowdhury,¹³⁴ P. Christakoglou,⁸⁸ C. H. Christensen,⁸⁷ P. Christiansen,⁷⁹
 T. Chujo,¹³³ C. Cicalo,⁵⁴ L. Cifarelli,^{10,27a,27b} F. Cindolo,⁵³ J. Cleymans,¹²⁴ F. Colamaria,⁵² D. Colella,⁵² A. Collu,⁷⁸
 M. Colocci,^{27a,27b} M. Concas,^{58a} G. Conesa Balbastre,⁷⁷ Z. Conesa del Valle,⁶¹ G. Contin,^{59,127} J. G. Contreras,³⁷
 T. M. Cormier,⁹⁴ Y. Corrales Morales,^{26a,26b,58} P. Cortese,³² M. R. Cosentino,¹²³ F. Costa,³⁴ S. Costanza,¹³⁹ J. Crkovská,⁶¹
 P. Crochet,¹³⁴ E. Cuautle,⁶⁹ L. Cunqueiro,⁹⁴ D. Dabrowski,¹⁴² T. Dahms,^{103,117} A. Dainese,⁵⁶ F. P. A. Damas,^{114,137} S. Dani,⁶⁵
 M. C. Danisch,¹⁰² A. Danu,⁶⁷ D. Das,¹⁰⁸ I. Das,¹⁰⁸ P. Das,^{3a,3b} S. Das,^{3a,3b} A. Dash,⁸⁴ S. Dash,⁴⁸ A. Dashi,¹⁰³ S. De,^{49,84}
 A. De Caro,^{30a,30b} G. de Cataldo,⁵² C. de Conti,¹²¹ J. de Cuveland,³⁹ A. De Falco,^{24a,24b} D. De Gruttola,¹⁰ N. De Marco,⁵⁸
 S. De Pasquale,^{30a,30b} R. D. De Souza,¹²² S. Deb,⁴⁹ H. F. Degenhardt,¹²¹ K. R. Deja,¹⁴² A. Deloff,⁸³ S. Delsanto,^{26a,26b,131}
 D. Devetak,¹⁰⁵ P. Dhankher,⁴⁸ D. Di Bari,^{33a,33b} A. Di Mauro,³⁴ R. A. Diaz,⁸ T. Dietel,¹²⁴ P. Dillenseger,⁶⁸ Y. Ding,⁶
 R. Divià,³⁴ Ø. Djuvsland,²² U. Dmitrieva,⁶² A. Dobrin,^{34,67} B. Dönigus,⁶⁸ O. Dordic,²¹ A. K. Dubey,¹⁴¹ A. Dubla,¹⁰⁵
 S. Dudi,⁹⁸ M. Dukhishyam,⁸⁴ P. Dupieux,¹³⁴ R. J. Ehlers,¹⁴⁶ D. Elia,⁵² H. Engel,⁷³ E. Epple,¹⁴⁶ B. Erazmus,¹¹⁴ F. Erhardt,⁹⁷
 A. Erokhin,¹¹² M. R. Ersdal,²² B. Espagnon,⁶¹ G. Eulisse,³⁴ J. Eum,¹⁸ D. Evans,¹⁰⁹ S. Evdokimov,⁸⁹ L. Fabbietti,^{103,117}
 M. Faggin,^{29a,29b} J. Faivre,⁷⁷ A. Fantoni,⁵¹ M. Fasel,⁹⁴ P. Fecchio,³¹ A. Feliciello,⁵⁸ G. Feofilov,¹¹² A. Fernández Téllez,⁴⁴
 A. Ferrero,¹³⁷ A. Ferretti,^{26a,26b} A. Festanti,³⁴ V. J. G. Feuillard,¹⁰² J. Figiel,¹¹⁸ S. Filchagin,¹⁰⁷ D. Finogeev,⁶² F. M. Fionda,²²
 G. Fiorenza,⁵² F. Flor,¹²⁵ S. Foertsch,⁷² P. Foka,¹⁰⁵ S. Fokin,⁸⁶ E. Fragiaco,⁵⁹ U. Frankenfeld,¹⁰⁵ G. G. Fronze,^{26a,26b}
 U. Fuchs,³⁴ C. Furget,⁷⁷ A. Furs,⁶² M. Fusco Girard,^{30a,30b} J. J. Gaardhøje,⁸⁷ M. Gagliardi,^{26a,26b} A. M. Gago,¹¹⁰ A. Gal,¹³⁶
 C. D. Galvan,¹²⁰ P. Ganoti,⁸² C. Garabatos,¹⁰⁵ E. Garcia-Solis,¹¹ K. Garg,^{28a,28b} C. Gargiulo,³⁴ A. Garibli,⁸⁵ K. Garner,¹⁴⁴
 P. Gasik,^{103,117} E. F. Gauger,¹¹⁹ M. B. Gay Ducati,⁷⁰ M. Germain,¹¹⁴ J. Ghosh,¹⁰⁸ P. Ghosh,¹⁴¹ S. K. Ghosh,^{3a,3b} P. Gianotti,⁵¹
 P. Giubellino,^{58,105} P. Giubileo,^{29a,29b} P. Glässel,¹⁰² D. M. Gómez Coral,⁷¹ A. Gomez Ramirez,⁷³ V. Gonzalez,¹⁰⁵
 P. González-Zamora,⁴⁴ S. Gorbunov,³⁹ L. Görlich,¹¹⁸ S. Gotovac,³⁵ V. Grabski,⁷¹ L. K. Graczykowski,¹⁴² K. L. Graham,¹⁰⁹
 L. Greiner,⁷⁸ A. Grelli,⁶³ C. Grigoras,³⁴ V. Grigoriev,⁹¹ A. Grigoryan,¹ S. Grigoryan,⁷⁴ O. S. Groettvik,²² J. M. Gronefeld,¹⁰⁵
 F. Grosa,³¹ J. F. Grosse-Oetringhaus,³⁴ R. Grosso,¹⁰⁵ R. Guernane,⁷⁷ B. Guerzoni,^{27a,27b} M. Guittiere,¹¹⁴ K. Gulbrandsen,⁸⁷
 T. Gunji,¹³² A. Gupta,⁹⁹ R. Gupta,⁹⁹ I. B. Guzman,⁴⁴ R. Haake,¹⁴⁶ M. K. Habib,¹⁰⁵ C. Hadjidakis,⁶¹ H. Hamagaki,⁸⁰
 G. Hamar,¹⁴⁵ M. Hamid,⁶ R. Hannigan,¹¹⁹ M. R. Haque,⁶³ A. Harlenderova,¹⁰⁵ J. W. Harris,¹⁴⁶ A. Harton,¹¹
 J. A. Hasenbichler,³⁴ H. Hassan,⁷⁷ D. Hatzifotiadou,^{10,53} P. Hauer,⁴² S. Hayashi,¹³² A. D. L. B. Hechavarria,¹⁴⁴
 S. T. Heckel,⁶⁸ E. Hellbär,⁶⁸ H. Helstrup,³⁶ A. Herghelegiu,⁴⁷ E. G. Hernandez,⁴⁴ G. Herrera Corral,⁹ F. Herrmann,¹⁴⁴
 K. F. Hetland,³⁶ T. E. Hilden,⁴³ H. Hillemanns,³⁴ C. Hills,¹²⁷ B. Hippolyte,¹³⁶ B. Hohlweger,¹⁰³ D. Horak,³⁷ S. Hornung,¹⁰⁵
 R. Hosokawa,^{16,133} P. Hristov,³⁴ C. Huang,⁶¹ C. Hughes,¹³⁰ P. Huhn,⁶⁸ T. J. Humanic,⁹⁵ H. Hushnud,¹⁰⁸ L. A. Husova,¹⁴⁴
 N. Hussain,⁴¹ S. A. Hussain,¹⁵ T. Hussain,¹⁷ D. Hutter,³⁹ D. S. Hwang,¹⁹ J. P. Iddon,^{34,127} R. Ilkaev,¹⁰⁷ M. Inaba,¹³³
 M. Ippolitov,⁸⁶ M. S. Islam,¹⁰⁸ M. Ivanov,¹⁰⁵ V. Ivanov,⁹⁶ V. Izucheev,⁸⁹ B. Jacak,⁷⁸ N. Jacazio,^{27a,27b} P. M. Jacobs,⁷⁸
 M. B. Jadhav,⁴⁸ S. Jadlovská,¹¹⁶ J. Jadlovsky,¹¹⁶ S. Jaelani,⁶³ C. Jahnke,¹²¹ M. J. Jakubowska,¹⁴² M. A. Janik,¹⁴² M. Jercic,⁹⁷
 O. Jevons,¹⁰⁹ R. T. Jimenez Bustamante,¹⁰⁵ M. Jin,¹²⁵ F. Jonas,^{94,144} P. G. Jones,¹⁰⁹ A. Jusko,¹⁰⁹ P. Kalinak,⁶⁴ A. Kalweit,³⁴
 J. H. Kang,¹⁴⁷ V. Kaplin,⁹¹ S. Kar,⁶ A. Karasu Uysal,⁷⁶ O. Karavichev,⁶² T. Karavicheva,⁶² P. Karczmarczyk,³⁴
 E. Karpechev,⁶² U. Kebschull,⁷³ R. Keidel,⁴⁶ M. Keil,³⁴ B. Ketzer,⁴² Z. Khabanova,⁸⁸ A. M. Khan,⁶ S. Khan,¹⁷
 S. A. Khan,¹⁴¹ A. Khanzadeev,⁹⁶ Y. Kharlov,⁸⁹ A. Khatun,¹⁷ A. Khuntia,^{49,118} B. Kileng,³⁶ B. Kim,⁶⁰ B. Kim,¹³³ D. Kim,¹⁴⁷
 D. J. Kim,¹²⁶ E. J. Kim,¹³ H. Kim,¹⁴⁷ J. Kim,¹⁴⁷ J. S. Kim,⁴⁰ J. Kim,¹⁰² J. Kim,¹⁴⁷ J. Kim,¹³ M. Kim,¹⁰² S. Kim,¹⁹ T. Kim,¹⁴⁷
 T. Kim,¹⁴⁷ S. Kirsch,³⁹ I. Kisel,³⁹ S. Kiselev,⁹⁰ A. Kisiel,¹⁴² J. L. Klay,⁵ C. Klein,⁶⁸ J. Klein,⁵⁸ S. Klein,⁷⁸ C. Klein-Bösing,¹⁴⁴

S. Klewin,¹⁰² A. Kluge,³⁴ M. L. Knichel,³⁴ A. G. Knospe,¹²⁵ C. Kobdaj,¹¹⁵ M. K. Köhler,¹⁰² T. Kollegger,¹⁰⁵
A. Kondratyev,⁷⁴ N. Kondratyeva,⁹¹ E. Kondratyuk,⁸⁹ P. J. Konopka,³⁴ L. Koska,¹¹⁶ O. Kovalenko,⁸³ V. Kovalenko,¹¹²
M. Kowalski,¹¹⁸ I. Králik,⁶⁴ A. Kravčáková,³⁸ L. Kreis,¹⁰⁵ M. Krivda,^{64,109} F. Krizek,⁹³ K. Krizkova Gajdosova,³⁷
M. Krüger,⁶⁸ E. Kryshen,⁹⁶ M. Krzewicki,³⁹ A. M. Kubera,⁹⁵ V. Kučera,⁶⁰ C. Kuhn,¹³⁶ P. G. Kuijjer,⁸⁸ L. Kumar,⁹⁸
S. Kumar,⁴⁸ S. Kundu,⁸⁴ P. Kurashvili,⁸³ A. Kurepin,⁶² A. B. Kurepin,⁶² A. Kuryakin,¹⁰⁷ S. Kushpil,⁹³ J. Kvapil,¹⁰⁹
M. J. Kweon,⁶⁰ J. Y. Kwon,⁶⁰ Y. Kwon,¹⁴⁷ S. L. La Pointe,³⁹ P. La Rocca,^{28a,28b} Y. S. Lai,⁷⁸ R. Langoy,¹²⁹ K. Lapidus,^{34,146}
A. Lardeux,²¹ P. Larionov,⁵¹ E. Laudi,³⁴ R. Lavicka,³⁷ T. Lazareva,¹¹² R. Lea,^{25a,25b} L. Leardini,¹⁰² S. Lee,¹⁴⁷ F. Lehas,⁸⁸
S. Lehner,¹¹³ J. Lehrbach,³⁹ R. C. Lemmon,⁹² I. León Monzón,¹²⁰ E. D. Lesser,²⁰ M. Lettrich,³⁴ P. Lévai,¹⁴⁵ X. Li,¹²
X. L. Li,⁶ J. Lien,¹²⁹ R. Lietava,¹⁰⁹ B. Lim,¹⁸ S. Lindal,²¹ V. Lindenstruth,³⁹ S. W. Lindsay,¹²⁷ C. Lippmann,¹⁰⁵ M. A. Lisa,⁹⁵
V. Litichevskyi,⁴³ A. Liu,⁷⁸ S. Liu,⁹⁵ W. J. Llope,¹⁴³ I. M. Lofnes,²² V. Loginov,⁹¹ C. Loizides,⁹⁴ P. Loncar,³⁵ X. Lopez,¹³⁴
E. López Torres,⁸ P. Luettig,⁶⁸ J. R. Luhder,¹⁴⁴ M. Lunardon,^{29a,29b} G. Luparello,⁵⁹ M. Lupi,⁷³ A. Maevskaya,⁶² M. Mager,³⁴
S. M. Mahmood,²¹ T. Mahmoud,⁴² A. Maire,¹³⁶ R. D. Majka,¹⁴⁶ M. Malaev,⁹⁶ Q. W. Malik,²¹ L. Malinina,^{74b}
D. Mal'Kevich,⁹⁰ P. Malzacher,¹⁰⁵ A. Mamonov,¹⁰⁷ G. Mandaglio,⁵⁵ V. Manko,⁸⁶ F. Manso,¹³⁴ V. Manzari,⁵² Y. Mao,⁶
M. Marchisone,¹³⁵ J. Mareš,⁶⁶ G. V. Margagliotti,^{25a,25b} A. Margotti,⁵³ J. Margutti,⁶³ A. Marín,¹⁰⁵ C. Markert,¹¹⁹
M. Marquard,⁶⁸ N. A. Martin,¹⁰² P. Martinengo,³⁴ J. L. Martinez,¹²⁵ M. I. Martínez,⁴⁴ G. Martínez García,¹¹⁴
M. Martinez Pedreira,³⁴ S. Masciocchi,¹⁰⁵ M. Maserà,^{26a,26b} A. Masoni,⁵⁴ L. Massacrier,⁶¹ E. Masson,¹¹⁴ A. Mastroserio,¹³⁸
A. M. Mathis,^{103,117} O. Matonoha,⁷⁹ P. F. T. Matuoka,¹²¹ A. Matyja,¹¹⁸ C. Mayer,¹¹⁸ M. Mazzilli,^{33a,33b} M. A. Mazzone,⁵⁷
A. F. Mechler,⁶⁸ F. Meddi,^{23a,23b} Y. Melikyan,⁹¹ A. Menchaca-Rocha,⁷¹ E. Meninno,^{30a,30b} M. Meres,¹⁴ S. Mhlanga,¹²⁴
Y. Miake,¹³³ L. Micheletti,^{26a,26b} M. M. Mieskolainen,⁴³ D. L. Mihaylov,¹⁰³ K. Mikhaylov,^{74,90} A. Mischke,^{63,†}
A. N. Mishra,⁶⁹ D. Miśkowiec,¹⁰⁵ C. M. Mitu,⁶⁷ A. Modak,^{3a,3b} N. Mohammadi,³⁴ A. P. Mohanty,⁶³ B. Mohanty,⁸⁴
M. Mohisin Khan,^{17c} M. Mondal,¹⁴¹ M. M. Mondal,⁶⁵ C. Mordasini,¹⁰³ D. A. Moreira De Godoy,¹⁴⁴ L. A. P. Moreno,⁴⁴
S. Moretto,^{29a,29b} A. Morreale,¹¹⁴ A. Morsch,³⁴ T. Mrnjavac,³⁴ V. Muccifora,⁵¹ E. Mudnic,³⁵ D. Mühlheim,¹⁴⁴ S. Muhuri,¹⁴¹
J. D. Mulligan,⁷⁸ M. G. Munhoz,¹²¹ K. Munning,⁴² R. H. Munzer,⁶⁸ H. Murakami,¹³² S. Murray,⁷² L. Musa,³⁴ J. Musinsky,⁶⁴
C. J. Myers,¹²⁵ J. W. Myrcha,¹⁴² B. Naik,⁴⁸ R. Nair,⁸³ B. K. Nandi,⁴⁸ R. Nania,^{10,53} E. Nappi,⁵² M. U. Naru,¹⁵
A. F. Nassirpour,⁷⁹ H. Natal da Luz,¹²¹ C. Nattrass,¹³⁰ R. Nayak,⁴⁸ T. K. Nayak,^{84,141} S. Nazarenko,¹⁰⁷
R. A. Negrao De Oliveira,⁶⁸ L. Nellen,⁶⁹ S. V. Nesbo,³⁶ G. Neskovic,³⁹ D. Nesterov,¹¹² B. S. Nielsen,⁸⁷ S. Nikolaev,⁸⁶
S. Nikulin,⁸⁶ V. Nikulin,⁹⁶ F. Noferini,^{10,53} P. Nomokonov,⁷⁴ G. Nooren,⁶³ J. Norman,⁷⁷ N. Novitzky,¹³³ P. Nowakowski,¹⁴²
A. Nyanin,⁸⁶ J. Nystrand,²² M. Ogino,⁸⁰ A. Ohlson,¹⁰² J. Oleniacz,¹⁴² A. C. Oliveira Da Silva,¹²¹ M. H. Oliver,¹⁴⁶
C. Oppedisano,⁵⁸ R. Orava,⁴³ A. Ortiz Velasquez,⁶⁹ A. Oskarsson,⁷⁹ J. Otwinowski,¹¹⁸ K. Oyama,⁸⁰ Y. Pachmayer,¹⁰²
V. Pacik,⁸⁷ D. Pagano,¹⁴⁰ G. Paić,⁶⁹ P. Palni,⁶ J. Pan,¹⁴³ A. K. Pandey,⁴⁸ S. Panebianco,¹³⁷ V. Papikyan,¹ P. Pareek,⁴⁹
J. Park,⁶⁰ J. E. Parkkila,¹²⁶ S. Parmar,⁹⁸ A. Passfeld,¹⁴⁴ S. P. Pathak,¹²⁵ R. N. Patra,¹⁴¹ B. Paul,^{24a,24b,58} H. Pei,⁶
T. Peitzmann,⁶³ X. Peng,⁶ L. G. Pereira,⁷⁰ H. Pereira Da Costa,¹³⁷ D. Peresunko,⁸⁶ G. M. Perez,⁸ E. Perez Lezama,⁶⁸
V. Peskov,⁶⁸ Y. Pestov,⁴ V. Petráček,³⁷ M. Petrovici,⁴⁷ R. P. Pezzi,⁷⁰ S. Piano,⁵⁹ M. Pikna,¹⁴ P. Pillot,¹¹⁴
L. O. D. L. Pimentel,⁸⁷ O. Pinazza,^{34,53} L. Pinsky,¹²⁵ C. Pinto,^{28a,28b} S. Pisano,⁵¹ D. Pistone,⁵⁵ D. B. Piyarathna,¹²⁵
M. Płoskoń,⁷⁸ M. Planinic,⁹⁷ F. Pliquett,⁶⁸ J. Pluta,¹⁴² S. Pochybova,¹⁴⁵ M. G. Poghosyan,⁹⁴ B. Polichtchouk,⁸⁹ N. Poljak,⁹⁷
W. Poonsawat,¹¹⁵ A. Pop,⁴⁷ H. Poppenborg,¹⁴⁴ S. Porteboeuf-Houssais,¹³⁴ V. Pozdniakov,⁷⁴ S. K. Prasad,^{3a,3b}
R. Preghenella,⁵³ F. Prino,⁵⁸ C. A. Pruneau,¹⁴³ I. Pshenichnov,⁶² M. Puccio,^{26a,26b,34} V. Punin,¹⁰⁷ K. Puranapanda,¹⁴¹
J. Putschke,¹⁴³ R. E. Quishpe,¹²⁵ S. Ragoni,¹⁰⁹ S. Raha,^{3a,3b} S. Rajput,⁹⁹ J. Rak,¹²⁶ A. Rakotozafindrabe,¹³⁷ L. Ramello,³²
F. Rami,¹³⁶ R. Raniwala,¹⁰⁰ S. Raniwala,¹⁰⁰ S. S. Räsänen,⁴³ B. T. Rascanu,⁶⁸ R. Rath,⁴⁹ V. Ratha,⁴² I. Ravasenga,³¹
K. F. Read,^{94,130} K. Redlich,^{83,d} A. Rehman,²² P. Reichelt,⁶⁸ F. Reidt,³⁴ X. Ren,⁶ R. Renfordt,⁶⁸ A. Reshetin,⁶² J.-P. Revol,¹⁰
K. Reygers,¹⁰² V. Riabov,⁹⁶ T. Richert,^{79,87} M. Richter,²¹ P. Riedler,³⁴ W. Riegler,³⁴ F. Riggi,^{28a,28b} C. Ristea,⁶⁷ S. P. Rode,⁴⁹
M. Rodríguez Cahuantzi,⁴⁴ K. Røed,²¹ R. Rogalev,⁸⁹ E. Rogochaya,⁷⁴ D. Rohr,³⁴ D. Röhrich,²² P. S. Rokita,¹⁴²
F. Ronchetti,⁵¹ E. D. Rosas,⁶⁹ K. Roslon,¹⁴² P. Rosnet,¹³⁴ A. Rossi,^{29a,29b} A. Rotondi,¹³⁹ F. Roukoutakis,⁸² A. Roy,⁴⁹
P. Roy,¹⁰⁸ O. V. Rueda,⁷⁹ R. Rui,^{25a,25b} B. Rumyantsev,⁷⁴ A. Rustamov,⁸⁵ E. Ryabinkin,⁸⁶ Y. Ryabov,⁹⁶ A. Rybicki,¹¹⁸
H. Rytönen,¹²⁶ S. Sadhu,¹⁴¹ S. Sadovsky,⁸⁹ K. Šafařík,^{34,37} S. K. Saha,¹⁴¹ B. Sahoo,⁴⁸ P. Sahoo,^{48,49} R. Sahoo,⁴⁹ S. Sahoo,⁶⁵
P. K. Sahu,⁶⁵ J. Saini,¹⁴¹ S. Sakai,¹³³ S. Sambyal,⁹⁹ V. Samsonov,^{91,96} F. R. Sanchez,⁴⁴ A. Sandoval,⁷¹ A. Sarkar,⁷²
D. Sarkar,¹⁴³ N. Sarkar,¹⁴¹ P. Sarma,⁴¹ V. M. Sarti,¹⁰³ M. H. P. Sas,⁶³ E. Scapparone,⁵³ B. Schaefer,⁹⁴ J. Schambach,¹¹⁹
H. S. Scheid,⁶⁸ C. Schiaua,⁴⁷ R. Schicker,¹⁰² A. Schmah,¹⁰² C. Schmidt,¹⁰⁵ H. R. Schmidt,¹⁰¹ M. O. Schmidt,¹⁰²
M. Schmidt,¹⁰¹ N. V. Schmidt,^{68,94} A. R. Schmier,¹³⁰ J. Schukraft,^{34,87} Y. Schutz,^{34,136} K. Schwarz,¹⁰⁵ K. Schweda,¹⁰⁵

- ²¹*Department of Physics, University of Oslo, Oslo, Norway*
- ²²*Department of Physics and Technology, University of Bergen, Bergen, Norway*
- ^{23a}*Dipartimento di Fisica dell'Università 'La Sapienza', Rome, Italy*
^{23b}*Sezione INFN, Rome, Italy*
- ^{24a}*Dipartimento di Fisica dell'Università, Cagliari, Italy*
^{24b}*Sezione INFN, Cagliari, Italy*
- ^{25a}*Dipartimento di Fisica dell'Università, Trieste, Italy*
^{25b}*Sezione INFN, Trieste, Italy*
- ^{26a}*Dipartimento di Fisica dell'Università, Turin, Italy*
^{26b}*Sezione INFN, Turin, Italy*
- ^{27a}*Dipartimento di Fisica e Astronomia dell'Università, Bologna, Italy*
^{27b}*Sezione INFN, Bologna, Italy*
- ^{28a}*Dipartimento di Fisica e Astronomia dell'Università, Catania, Italy*
^{28b}*Sezione INFN, Catania, Italy*
- ^{29a}*Dipartimento di Fisica e Astronomia dell'Università, Padova, Italy*
^{29b}*Sezione INFN, Padova, Italy*
- ^{30a}*Dipartimento di Fisica 'E.R. Caianiello' dell'Università, Salerno, Italy*
^{30b}*Gruppo Collegato INFN, Salerno, Italy*
- ³¹*Dipartimento DISAT del Politecnico and Sezione INFN, Turin, Italy*
- ³²*Dipartimento di Scienze e Innovazione Tecnologica dell'Università del Piemonte Orientale and INFN Sezione di Torino, Alessandria, Italy*
^{33a}*Dipartimento Interateneo di Fisica 'M. Merlin', Bari, Italy*
^{33b}*Sezione INFN, Bari, Italy*
- ³⁴*European Organization for Nuclear Research (CERN), Geneva, Switzerland*
- ³⁵*Faculty of Electrical Engineering, Mechanical Engineering and Naval Architecture, University of Split, Split, Croatia*
- ³⁶*Faculty of Engineering and Science, Western Norway University of Applied Sciences, Bergen, Norway*
- ³⁷*Faculty of Nuclear Sciences and Physical Engineering, Czech Technical University in Prague, Czech Republic*
³⁸*Faculty of Science, P.J. Šafárik University, Košice, Slovakia*
- ³⁹*Frankfurt Institute for Advanced Studies, Johann Wolfgang Goethe-Universität Frankfurt, Frankfurt, Germany*
- ⁴⁰*Gangneung-Wonju National University, Gangneung, Republic of Korea*
- ⁴¹*Gauhati University, Department of Physics, Guwahati, India*
- ⁴²*Helmholtz-Institut für Strahlen- und Kernphysik, Rheinische Friedrich-Wilhelms-Universität Bonn, Bonn, Germany*
⁴³*Helsinki Institute of Physics (HIP), Helsinki, Finland*
- ⁴⁴*High Energy Physics Group, Universidad Autónoma de Puebla, Puebla, Mexico*
⁴⁵*Hiroshima University, Hiroshima, Japan*
- ⁴⁶*Hochschule Worms, Zentrum für Technologietransfer und Telekommunikation (ZTT), Worms, Germany*
- ⁴⁷*Horia Hulubei National Institute of Physics and Nuclear Engineering, Bucharest, Romania*
- ⁴⁸*Indian Institute of Technology Bombay (IIT), Mumbai, India*
⁴⁹*Indian Institute of Technology Indore, Indore, India*
- ⁵⁰*Indonesian Institute of Sciences, Jakarta, Indonesia*
- ⁵¹*INFN, Laboratori Nazionali di Frascati, Frascati, Italy*
⁵²*INFN, Sezione di Bari, Bari, Italy*
⁵³*INFN, Sezione di Bologna, Bologna, Italy*
⁵⁴*INFN, Sezione di Cagliari, Cagliari, Italy*
⁵⁵*INFN, Sezione di Catania, Catania, Italy*
⁵⁶*INFN, Sezione di Padova, Padova, Italy*
⁵⁷*INFN, Sezione di Roma, Rome, Italy*
⁵⁸*INFN, Sezione di Torino, Turin, Italy*
⁵⁹*INFN, Sezione di Trieste, Trieste, Italy*
⁶⁰*Inha University, Republic of Korea*
- ⁶¹*Institut de Physique Nucléaire d'Orsay (IPNO), Institut National de Physique Nucléaire et de Physique des Particules (IN2P3/CNRS), Université de Paris-Sud, Université Paris-Saclay, Orsay, France*
- ⁶²*Institute for Nuclear Research, Academy of Sciences, Moscow, Russia*
- ⁶³*Institute for Subatomic Physics, Utrecht University/Nikhef, Utrecht, Netherlands*
- ⁶⁴*Institute of Experimental Physics, Slovak Academy of Sciences, Košice, Slovakia*
- ⁶⁵*Institute of Physics, Homi Bhabha National Institute, Bhubaneswar, India*
- ⁶⁶*Institute of Physics of the Czech Academy of Sciences, Prague, Czech Republic*
⁶⁷*Institute of Space Science (ISS), Bucharest, Romania*
- ⁶⁸*Institut für Kernphysik, Johann Wolfgang Goethe-Universität Frankfurt, Frankfurt, Germany*
- ⁶⁹*Instituto de Ciencias Nucleares, Universidad Nacional Autónoma de México, Mexico City, Mexico*

- ⁷⁰*Instituto de Física, Universidade Federal do Rio Grande do Sul (UFRGS), Porto Alegre, Brazil*
- ⁷¹*Instituto de Física, Universidad Nacional Autónoma de México, Mexico City, Mexico*
- ⁷²*iThemba LABS, National Research Foundation, Somerset West, South Africa*
- ⁷³*Johann-Wolfgang-Goethe Universität Frankfurt Institut für Informatik, Fachbereich Informatik und Mathematik, Frankfurt, Germany*
- ⁷⁴*Joint Institute for Nuclear Research (JINR), Dubna, Russia*
- ⁷⁵*Korea Institute of Science and Technology Information, Daejeon, Republic of Korea*
- ⁷⁶*KTO Karatay University, Konya, Turkey*
- ⁷⁷*Laboratoire de Physique Subatomique et de Cosmologie, Université Grenoble-Alpes, CNRS-IN2P3, Grenoble, France*
- ⁷⁸*Lawrence Berkeley National Laboratory, Berkeley, California, United States*
- ⁷⁹*Lund University Department of Physics, Division of Particle Physics, Lund, Sweden*
- ⁸⁰*Nagasaki Institute of Applied Science, Nagasaki, Japan*
- ⁸¹*Nara Women's University (NWU), Nara, Japan*
- ⁸²*National and Kapodistrian University of Athens, School of Science, Department of Physics, Athens, Greece*
- ⁸³*National Centre for Nuclear Research, Warsaw, Poland*
- ⁸⁴*National Institute of Science Education and Research, Homi Bhabha National Institute, Jatni, India*
- ⁸⁵*National Nuclear Research Center, Baku, Azerbaijan*
- ⁸⁶*National Research Centre Kurchatov Institute, Moscow, Russia*
- ⁸⁷*Niels Bohr Institute, University of Copenhagen, Copenhagen, Denmark*
- ⁸⁸*Nikhef, National institute for subatomic physics, Amsterdam, Netherlands*
- ⁸⁹*NRC Kurchatov Institute IHEP, Protvino, Russia*
- ⁹⁰*NRC «Kurchatov Institute»—ITEP, Moscow, Russia*
- ⁹¹*NRNU Moscow Engineering Physics Institute, Moscow, Russia*
- ⁹²*Nuclear Physics Group, STFC Daresbury Laboratory, United Kingdom*
- ⁹³*Nuclear Physics Institute of the Czech Academy of Sciences, Řež u Prahy, Czech Republic*
- ⁹⁴*Oak Ridge National Laboratory, Oak Ridge, Tennessee, United States*
- ⁹⁵*Ohio State University, Columbus, Ohio, United States*
- ⁹⁶*Petersburg Nuclear Physics Institute, Gatchina, Russia*
- ⁹⁷*Physics department, Faculty of science, University of Zagreb, Zagreb, Croatia*
- ⁹⁸*Physics Department, Panjab University, Chandigarh, India*
- ⁹⁹*Physics Department, University of Jammu, Jammu, India*
- ¹⁰⁰*Physics Department, University of Rajasthan, Jaipur, India*
- ¹⁰¹*Physikalisches Institut, Eberhard-Karls-Universität Tübingen, Tübingen, Germany*
- ¹⁰²*Physikalisches Institut, Ruprecht-Karls-Universität Heidelberg, Heidelberg, Germany*
- ¹⁰³*Physik Department, Technische Universität München, Munich, Germany*
- ¹⁰⁴*Politecnico di Bari, Bari, Italy*
- ¹⁰⁵*Research Division and ExtreMe Matter Institute EMMI, GSI Helmholtzzentrum für Schwerionenforschung GmbH, Bari, Italy*
- ¹⁰⁶*Rudjer Bošković Institute, Zagreb, Croatia*
- ¹⁰⁷*Russian Federal Nuclear Center (VNIIEF), Sarov, Russia*
- ¹⁰⁸*Saha Institute of Nuclear Physics, Homi Bhabha National Institute, Kolkata, India*
- ¹⁰⁹*School of Physics and Astronomy, University of Birmingham, Birmingham, United Kingdom*
- ¹¹⁰*Sección Física, Departamento de Ciencias, Pontificia Universidad Católica del Perú, Lima, Peru*
- ¹¹¹*Shanghai Institute of Applied Physics, Shanghai, China*
- ¹¹²*St. Petersburg State University, St. Petersburg, Russia*
- ¹¹³*Stefan Meyer Institut für Subatomare Physik (SMI), Vienna, Austria*
- ¹¹⁴*SUBATECH, IMT Atlantique, Université de Nantes, CNRS-IN2P3, Nantes, France*
- ¹¹⁵*Suranaree University of Technology, Nakhon Ratchasima, Thailand*
- ¹¹⁶*Technical University of Košice, Košice, Slovakia*
- ¹¹⁷*Technische Universität München, Excellence Cluster 'Universe', Munich, Germany*
- ¹¹⁸*The Henryk Niewodniczanski Institute of Nuclear Physics, Polish Academy of Sciences, Cracow, Poland*
- ¹¹⁹*The University of Texas at Austin, Austin, Texas, United States*
- ¹²⁰*Universidad Autónoma de Sinaloa, Culiacán, Mexico*
- ¹²¹*Universidade de São Paulo (USP), São Paulo, Brazil*
- ¹²²*Universidade Estadual de Campinas (UNICAMP), Campinas, Brazil*
- ¹²³*Universidade Federal do ABC, Santo Andre, Brazil*
- ¹²⁴*University of Cape Town, Cape Town, South Africa*
- ¹²⁵*University of Houston, Houston, Texas, United States*
- ¹²⁶*University of Jyväskylä, Jyväskylä, Finland*
- ¹²⁷*University of Liverpool, Liverpool, United Kingdom*
- ¹²⁸*University of Science and Technology of China, Hefei, China*
- ¹²⁹*University of South-Eastern Norway, Tonsberg, Norway*

¹³⁰*University of Tennessee, Knoxville, Tennessee, United States*

¹³¹*University of the Witwatersrand, Johannesburg, South Africa*

¹³²*University of Tokyo, Tokyo, Japan*

¹³³*University of Tsukuba, Tsukuba, Japan*

¹³⁴*Université Clermont Auvergne, CNRS/IN2P3, LPC, Clermont-Ferrand, France*

¹³⁵*Université de Lyon, Université Lyon 1, CNRS/IN2P3, IPN-Lyon, Villeurbanne, Lyon, France*

¹³⁶*Université de Strasbourg, CNRS, IPHC UMR 7178, F-67000 Strasbourg, France, Strasbourg, France*

¹³⁷*Université Paris-Saclay Centre d'Etudes de Saclay (CEA), IRFU, Département de Physique Nucléaire (DPn), Saclay, France*

¹³⁸*Università degli Studi di Foggia, Foggia, Italy*

¹³⁹*Università degli Studi di Pavia, Pavia, Italy*

¹⁴⁰*Università di Brescia, Brescia, Italy*

¹⁴¹*Variable Energy Cyclotron Centre, Homi Bhabha National Institute, Kolkata, India*

¹⁴²*Warsaw University of Technology, Warsaw, Poland*

¹⁴³*Wayne State University, Detroit, Michigan, United States*

¹⁴⁴*Westfälische Wilhelms-Universität Münster, Institut für Kernphysik, Münster, Germany*

¹⁴⁵*Wigner Research Centre for Physics, Hungarian Academy of Sciences, Budapest, Hungary*

¹⁴⁶*Yale University, New Haven, Connecticut, United States*

¹⁴⁷*Yonsei University, Seoul, Republic of Korea*

[†]Deceased.

^aAlso at Dipartimento DET del Politecnico di Torino, Turin, Italy.

^bAlso at M.V. Lomonosov Moscow State University, D.V. Skobeltsyn Institute of Nuclear Physics, Moscow, Russia.

^cAlso at Department of Applied Physics, Aligarh Muslim University, Aligarh, India.

^dAlso at Institute of Theoretical Physics, University of Wrocław, Poland.